Environ Sci Pollut Res (2014) 21:6671–6686
DOI 10.1007/s11356-014-2582-8

RESEARCH ARTICLE

Effect of ethanol addition on soot precursors emissions during benzene oxidation in a jet-stirred reactor

Yacine Rezgui · Miloud Guemini

Received: 17 July 2013 / Accepted: 21 January 2014 / Published online: 9 February 2014

Abstract A constant volume reactor model (PSR) was used to investigate the effect of ethanol addition on the formation of some pollutants during benzene oxidation in a jet-stirred reactor. The blended fuels were formed by incrementally adding 4 % wt of oxygen (ethanol) to the neat benzene fuel and by keeping the inert mole fraction (nitrogen) and the equivalence ratio constants. The main objective of this work was to obtain fundamental understanding of the mechanisms through which the oxygenate compound affects soot precursor amounts. The modeling results showed that C_2H_2, C_5H_5, and C_3H_3 mole fractions decreased upon increasing the ethanol percentage in the fuel mixture.

Keywords Ethanol · Oxygenated products · Soot precursors · JSR · Benzene · Modeling

Introduction

Nowadays, the reduction of the greenhouse gas emissions as well as the local pollution and the diversification of the energy sources for the transport are impelling the research of renewable and alternative cleaner fuels (Esarte et al. 2012; Frassoldati et al. 2012; Huang et al. 2007; Palit et al. 2011; Pidol et al. 2012; Sukjit et al. 2012). In this context, several government initiatives have been implemented at the regional, national, and local levels to help promote the development and expansion of alternative transportation fuels (Delshad et al. 2010). These initiatives have also been supported by regulatory organizations and environmental agencies who considered alternative transport fuels such as hydrogen, natural gas, Fischer–Tropsch fuels, and biofuels as a viable option to reduce the transport sector contribution to local air pollution (Karavalakis et al. 2012; Knothe 2010).

The most common biofuels are the biodiesel (esters) and bioalcohols; both of them can be implemented on existing combustion devices and can be used as alternative fuel substitutes, or as fuel additives (Balat et al. 2008; Johnson and Goldsborough 2009; Kohse-Hoinghaus et al. 2010; Salamanca et al. 2012). However, it is not yet clear which biofuels will emerge as the best possible choices for spark-ignition and compression-ignition engines nor indeed for gas turbines (Black et al. 2010).

Among the different bioalcohols, ethanol is one of the most studied and used oxygenated additive because it can be produced from agricultural products and scrapped resources. Also it is a biodegradable and an environmentally friendly alternative fuel (Yoon and Lee 2012). Due to these numerous benefits, bioethanol and ethanol–gasoline blends are widely used and investigated as alternative fuels in automotive vehicles (Francisco and Ahmad 2006; Marriott et al. 2008; Sayin and Uslu 2008; Yoon and Lee 2012; Yoon et al. 2008a, b), and consequently, the oxidation and combustion chemistry of ethanol and its blends with other hydrocarbons is of particular interest. In this context, several studies have been carried out in different combustion systems from lab-scale systems, including shock tubes, flow reactors, and others (Alexiou and Williams 1996; Böhm and Braun-Unkhoff 2008; Bennett et al. 2009; Fieweger et al. 1997; Lin et al. 2010; Litzinger et al. 2009; Parag and Raghavan 2009; Veloo et al. 2010), to real engines (Agarwal 2007; Arslan et al. 2012; Celik 2008; Guo et al. 2011; He et al. 2003; Huang et al. 2009; Keskin and Gürü 2011; Lapuerta et al. 2008; Liang et al. 2011; Maricq et al. 2012; Zhu et al. 2010), and detailed chemical mechanisms for ethanol–hydrocarbon fuels, which are useful for the design of well-

Responsible editor: Gerhard Lammel

Y. Rezgui (✉) · M. Guemini
Laboratoire de Chimie Appliquée et Technologie des Matériaux, Université d'Oum El Bouaghi, B.P. 358, Route de Constantine, Oum El Bouaghi 04000, Algeria
e-mail: yacinereference@yahoo.com

performing engines, have been extensively developed covering a wide range of engine operating conditions (Frassoldati et al. 2010; Li et al. 2001, 2007; Marinov 1999). It is noteworthy that even if in some cases the correlations between some fuel components and some pollutants were studied, the detailed correlations between each fuel component and each pollutant individual hydrocarbon are not presented yet.

The objective of the given study is to investigate the mechanism of ethanol influence on pollutants formation in a perfectly stirred reactor by studying the structure of benzene fuel with and without ethanol addition. This investigation is mainly focused on the modeling between the emitted pollutants and fuel composition as well as on the formation–consumption pathways of these pollutants.

Selected compounds

Benzene

The understanding of the oxidation of aromatic compounds has recently become one of the most interesting research subjects in the combustion society, from a fundamental point of view as well as from a practical point of view (Tan and Frank 1996). Aromatic compounds are known to be harmful to the environment, and the emission of these species from a number of combustion systems is a significant concern. Furthermore, aromatic species are important precursors to dioxins and to soot formation (Alzueta et al. 2000).

Due to its high density and antiknock rating, the simplest aromatic hydrocarbon, benzene, forms a considerable percentage in fuels, especially in unleaded gasoline. Besides, it is an important product during combustion processes, and its emissions are of major concern not only due to their toxicity but also because they lead to the formation of other toxic compounds upon oxidation. Due to these facts, benzene was chosen, in this work, as a representative for aromatic fuels.

Acetylene, cyclopentadienyl, and propargyl radicals

Several polycyclic aromatic hydrocarbons (PAHs) formed from incomplete combustion are known to be mutagenic or carcinogenic (Kim et al. 2007). It is generally believed that, under fuel-rich conditions, a two-step process involving hydrogen abstraction to activate the aromatic molecule followed by subsequent acetylene addition was the sequence responsible for the PAH molecular mass growth. The repetition of the sequence H abstraction followed by acetylene addition leads to the cyclization to the next higher-order ring (HACA mechanism) (Frenklach and Warnatz 1987; Wang and Frenklach 1997; Wang et al. 2006).

Early models based on the HACA mechanism, however, seem to be too slow to kinetically explain the formation of large PAHs (Appel et al. 2000; Wang et al. 2006; Yoon et al. 2008a, b), and alternatively recent studies have emphasized the potential importance of resonantly stabilized free radicals, such as propargyl (Hwang et al. 1998; Miller and Melius 1992) and cyclopentadienyl (Melius et al. 1996; Yang et al. 2006) in forming aromatics and PAHs.

As mentioned by Lee et al. (2004), the propargyl recombination reaction has been suggested as one of the dominant pathways for benzene formation (Miller and Melius 1992; Yoon et al. 2008a, b), and the role of odd carbon chemistries related to propargyl radicals has been emphasized for PAH growth (Lee et al. 2004). On the other hand, the cyclopentadienyl is considered to be an important intermediate in PAH formation due to its neutrality and ambident reactivity at different sites (McEnally and Pfefferle 1998). Due to the pertinent role of C_2H_2, C_3H_3, and C_5H_5 in forming aromatics and PAHs, these species were selected in our work.

Methodology

Improved mechanistic understanding and increasing availability of reliable thermodynamic and kinetic data, together with the fast evolution of computer hardware, have rendered kinetic modeling, a valuable tool for the quantitative assessment of combustion processes. In our case, kinetic modeling was conducted using the PSR code from the CHEMKIN II package (Glarborg et al. 1986).

The core of the reaction mechanism, used to describe pyrolysis and oxidation of the benzene, was gathered from the work of Vourliotakis et al. (2011). As mentioned by the authors, the proposed mechanism has been extensively validated against experimental speciation data from counterflow and premixed flames, including laminar flame speeds (Bittner and Howard 1981; Defoeux et al. 2005; Detilleux and Vandooren 2009; Yang et al. 2007); shock tubes, including ignition time delays (Burcat et al. 1986); and perfectly stirred and plug-flow reactors (Alzueta et al. 1998, 2000; Chai and Pfefferle 1998; Emdee et al. 1992; Lovell et al. 1989; Ristori et al. 2001), all under a wide range of temperatures, pressures, and stoichiometries. Predictive capabilities of the model were found to be at least fair and often good to excellent for the consumption of the reactants, the formation of the main combustion products, and the formation and depletion of major intermediates including radicals and oxygenated products.

To model the ethanol oxidation, additional reactions were added to the core mechanism from Marinov's (1999) model. The selected reactions from the alcohol kinetic scheme were the initial reactions of the molecules themselves such as hydrogen abstraction and unimolecular decomposition, as well as reactions of the resulting products that eventually produced species present in the benzene mechanism.

The ethanol mechanism developed by Marinov (1999) has been validated against a variety of experimental data sets (Aboussi 1991; Dunphy and Simmie 1991; Gulder 1982; Norton and Dryer 1992). The model is shown to successfully reproduce ethanol experimental data covering a wide range of operating conditions. Furthermore, it should be mentioned that the required input data were obtained via the combination of the thermodynamic data of the two studied species and that within the combined mechanism, all reactions and values of the rate coefficients were kept unchanged as compared to those in the base mechanisms. The combined mechanism is composed of 127 species and 863 reactions.

Finally, it is noteworthy that the neat benzene fuel has been previously studied experimentally by Ristori et al. (2001) in a jet-stirred reactor having a volume of 30.5 cm^3. The experimental conditions were atmospheric pressure, temperature ranging from 900 to 1,350 K, and residence time equal to 0.07 s. The blended fuels were formed by incrementally adding 4 % wt of oxygen (ethanol) to the neat benzene fuel and by keeping the inert mole fraction (nitrogen) and the equivalence ratio constants (see Table 1).

Results and discussion

Mechanism validation

In order to assess the predictive capability of the elaborated global mechanism in the perfectly stirred reactor conditions, experimental data from the study of Ristori et al. (2001) and Aboussi (1991) were compared with corresponding model predictions. Figure 1a–d shows the comparisons between predictions and experimental data (Ristori et al. 2001) carried out in a jet-stirred reactor in the temperature range 900–1,300 K, at a pressure of 1 atm, a residence time of 0.07 s, and a reactor volume of 30.5 cm^3. Results for the lean conditions ($\Phi=0.3$ and $\Phi=0.5$) are shown in Fig. 1a, b, where it can be seen that the reactivities of C_6H_6, O_2, and CH_2O are well predicted by the model whereas the CO_2 and c-C_5H_6 predicted reactivities are slightly more important than the measured ones. On the other hand, C_2H_2 is well predicted at low temperatures (temperature range 900–1,100 K), whereas its measured reactivity is more important than the calculated one for temperatures higher than 1,100 K. Underpredictions of more than a factor of 5.5, 5, and 3 are observed for CH_4, C_2H_6, and C_2H_4, respectively, in the case of $\Phi=0.3$ (Fig. 1a) and more than a factor of 3.6, 1.8, and 3.2 for the same species, respectively, in the case of $\Phi=0.5$ (Fig. 1b). Besides, the model accurately captures the mole fraction shape of a-C_3H_4; however, it underestimates p-C_3H_4 and C_4H_6 concentrations. Similar trends are observed in the case of an equivalence ratio equal to 0.5.

In the case of the stoichiometric conditions (Fig. 1c), a perfect matching in the C_6H_6, O_2, CO, CO_2, C_2H_2, and p-C_3H_4 levels was obtained. Also, the model captures the behavior of CH_2O reasonably well, although the simulated CH_2O profile was found to be slowly disappearing in the temperature range 1,250–1,300 K, as compared to the measured one. However, the model slightly underpredicts CH_4, C_2H_4, C_2H_6, and C_3H_6 levels. The greatest disagreement is observed in the case of C_4H_6, which the model underpredicts by a factor of 12.

For the fuel-rich conditions ($\Phi=1.5$), the used model describes well the concentration profiles of reactants (C_6H_6 and O_2) and of the main oxidation products (CO, CO_2, and H_2). For the intermediate products, a satisfactory agreement between experiments and calculations is observed for CH_4, C_2H_2, and C_2H_4, whereas a fair difference is observed for C_2H_6 and C_3H_6, which are underpredicted by the model by a factor of 1.6 and 4.4 for C_2H_6 and C_3H_6, respectively. Besides, the model predicts well the a-C_3H_4 level and overpredicts the p-C_3H_4 concentration. In addition, the used mechanism underpredicts the C_4H_4 and C_4H_6 mole fractions.

In order to verify the capability of the model to reproduce the ethanol and subsequent species depletion formation, the combined mechanism was tested in comparison with neat ethanol fuel oxidation measurements (Aboussi 1991). The experimental study was performed in an atmospheric jet-stirred reactor, at a temperature varying from 1,000 to 1,200 K, for equivalence ratios from 0.2 to 2 and ethanol concentration of 0.3 %. Measurements were taken as a function of residence time for CO, CO_2, CH_4, C_2H_4, C_2H_6, CH_3HCO, and C_2H_5OH (Aboussi 1991). The modeling results show that, in the case of the stoichiometric fuel, the reactivity of ethanol and of carbon dioxide is well predicted by the model (Fig. 2a). The maximum concentration of CO is overpredicted by a factor of 1.36, whereas the maximum concentration of C_2H_4 is underpredicted by a factor of 1.65. In addition, a good agreement is found between calculations and measurements in the case of CH_4, whereas a fair disagreement is found between the

Table 1 Parameters of the used ethanol–benzene fuels

Fuel	Composition (mole fractions)			
	C_6H_6	C_2H_5OH	O_2	N_2
Neat benzene fuel	0.001500	0.0000000	0.0225000	0.9760
Fuel with 4 % ethanol	0.001368	0.0003014	0.0223304	0.9760
Fuel with 8 % ethanol	0.0012279	0.0006219	0.0221501	0.9760
Fuel with 12 % ethanol	0.0010785	0.0009632	0.0219581	0.9760
Fuel with 16 % ethanol	0.0009191	0.0013276	0.0217531	0.9760
Fuel with 20 % ethanol	0.0007486	0.0017174	0.0215339	0.9760
Fuel with 24 % ethanol	0.0005657	0.0021353	0.0212988	0.9760

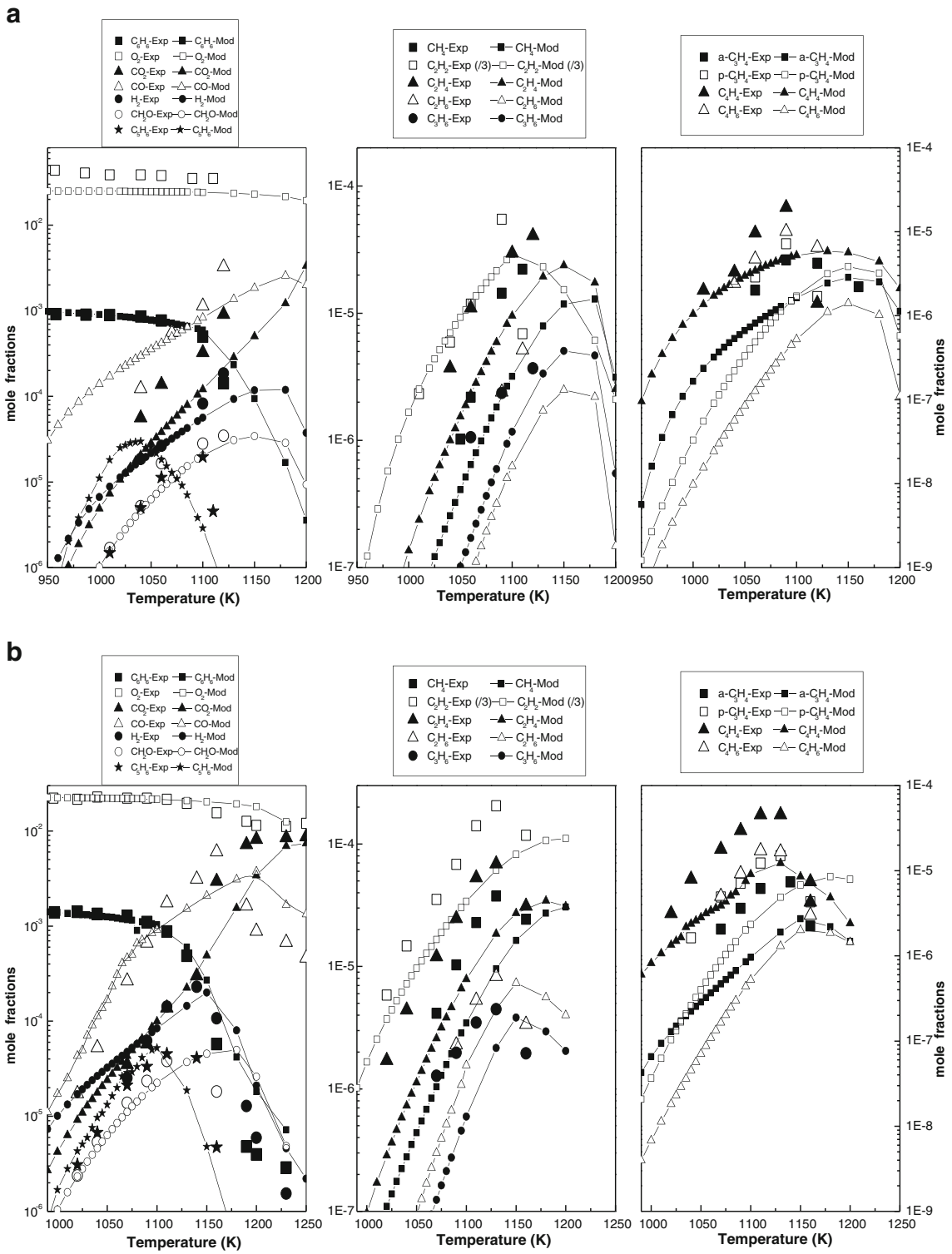

Fig. 1 **a** Experimental (*symbols*) and computed (*lines* and *small symbols*) species profiles in $C_6H_6/O_2/N_2$ fuel. Initial conditions: C_6H_6 0.1 %, O_2 2.5 %, N_2 97.4 %, and φ=0.3. **b** Experimental (*symbols*) and computed (*lines* and *small symbols*) species profiles in $C_6H_6/O_2/N_2$ fuel. Initial conditions: C_6H_6 0.15 %, O_2 2.25 %, N_2 97.6 %, and φ=0.5. **c** Experimental (*symbols*) and computed (*lines* and *small symbols*) species profiles in $C_6H_6/O_2/N_2$ fuel. Initial conditions: C_6H_6 0.15 %, O_2 1.125 %, N_2 98.725 %, and φ=1. **d** Experimental (*symbols*) and computed (*lines* and *small symbols*) species profiles in $C_6H_6/O_2/N_2$ fuel. Initial conditions: C_6H_6 0.15 %, O_2 0.75 %, N_2 99.1 %, and φ=1.5

model values and the measured ones in the case of C_2H_6 and CH_3CHO. On the other hand, in the case of the fuel-rich ethanol conditions (Fig. 2b), the model performs well in predicting the C_2H_5OH and C_2H_4 mole

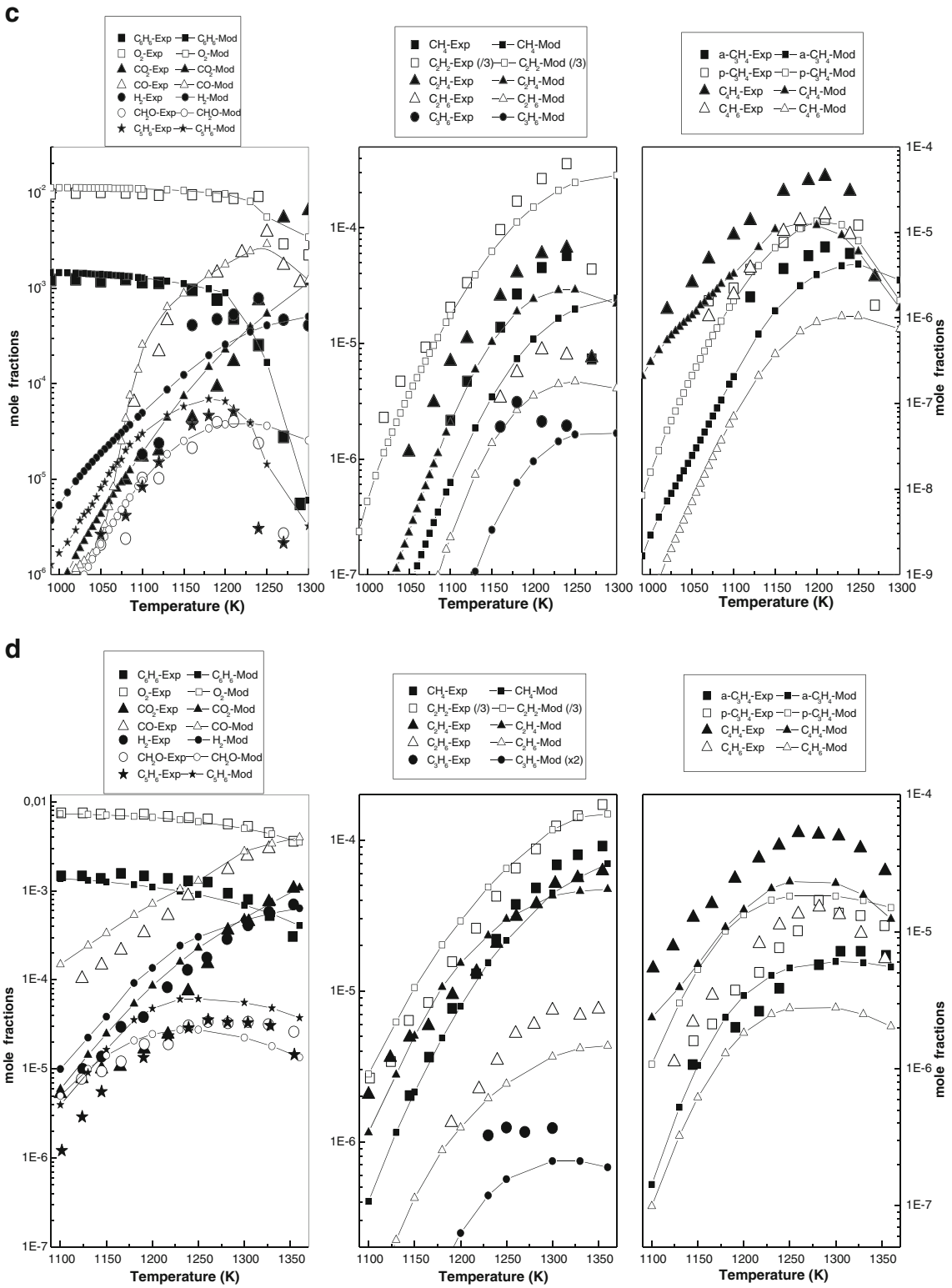

Fig. 1 (continued)

fractions, whereas it slightly underpredicts the CO_2 and CH_3CHO levels. Besides, the combined mechanism moderately underpredicts CO, CH_4, and C_2H_6 concentrations. To resume, it could be said that the model was able to accurately predict the main concentration profiles, either in the case of the benzene fuel or in the case of the ethanol fuel.

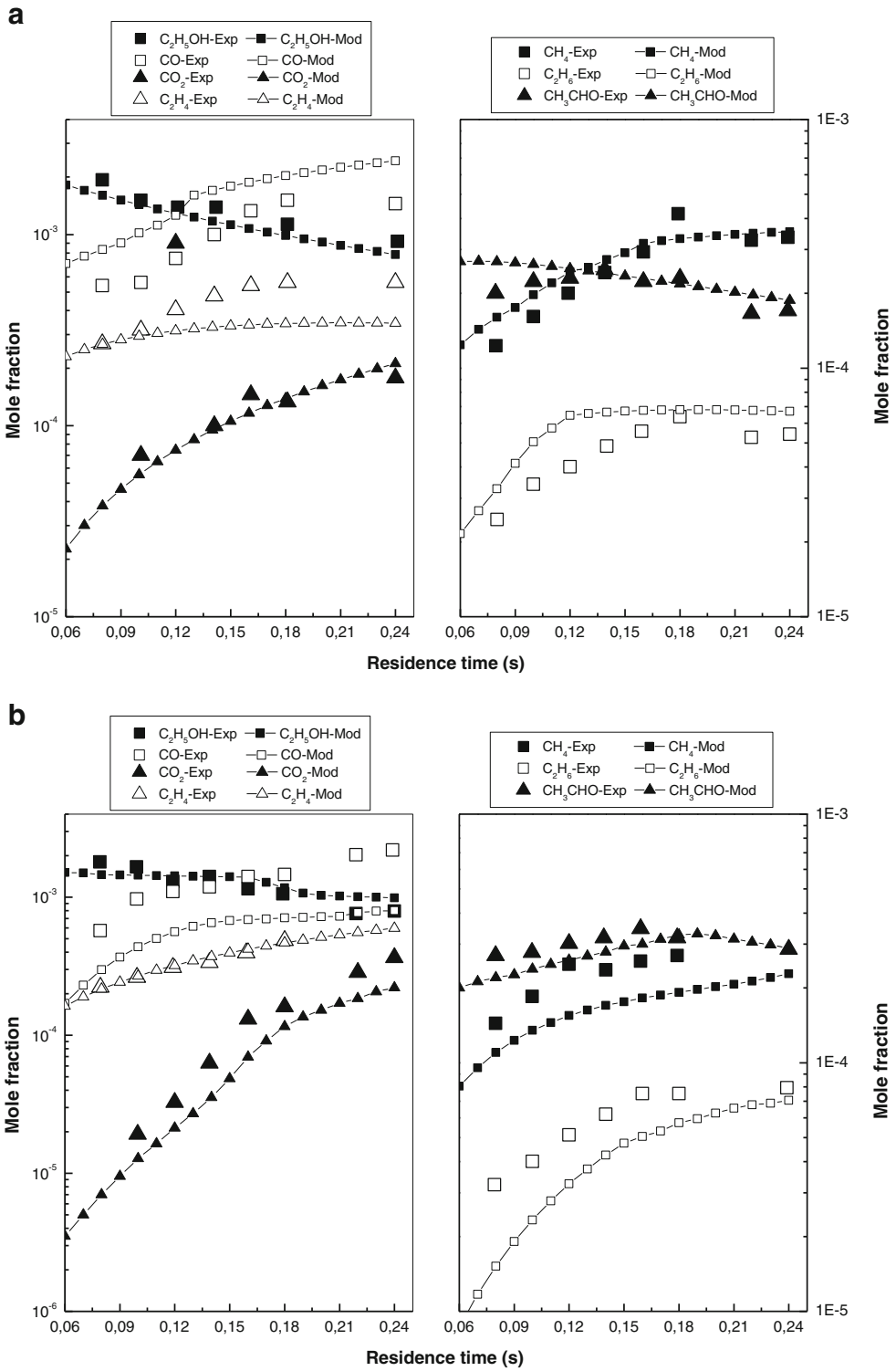

Fig. 2 **a** Experimental (*symbols*) and computed (*lines* and *small symbols*) species profiles in $C_2H_5OH/O_2/N_2$ fuel. Initial conditions: C_2H_5OH 0.3 %, O_2 0.9 %, N_2 98.8 %, 1.0 atmosphere, T=1,056 K, and φ= 1.0. **b** Experimental (*symbols*) and computed (*lines* and *small symbols*) species profiles in $C_2H_5OH/O_2/N_2$ fuel. Initial conditions: C_2H_5OH 0.3 %, O_2 0.45 %, N_2 99.25 %, 1.0 atmosphere, T=1,070 K, and φ= 2.0

Acetylene

The dependence of acetylene mole fractions on ethanol proportion in the fuel mixture is depicted in Fig. 3a. It can be seen that, regardless of the reaction temperature, the concentration of acetylene decreased upon increasing the percentage of the ethanol in the mixture. However, this decrease was dependent on the reaction temperature: 1,250 K exhibited the highest lowering (54.2 %), whereas 1,000 K displayed the lowest one (36.8 %). Similar trends were observed by Chen et al. (2013) during their study on the influences of methanol on premixed fuel-rich *n*-heptane flames, where it was mentioned that, at a

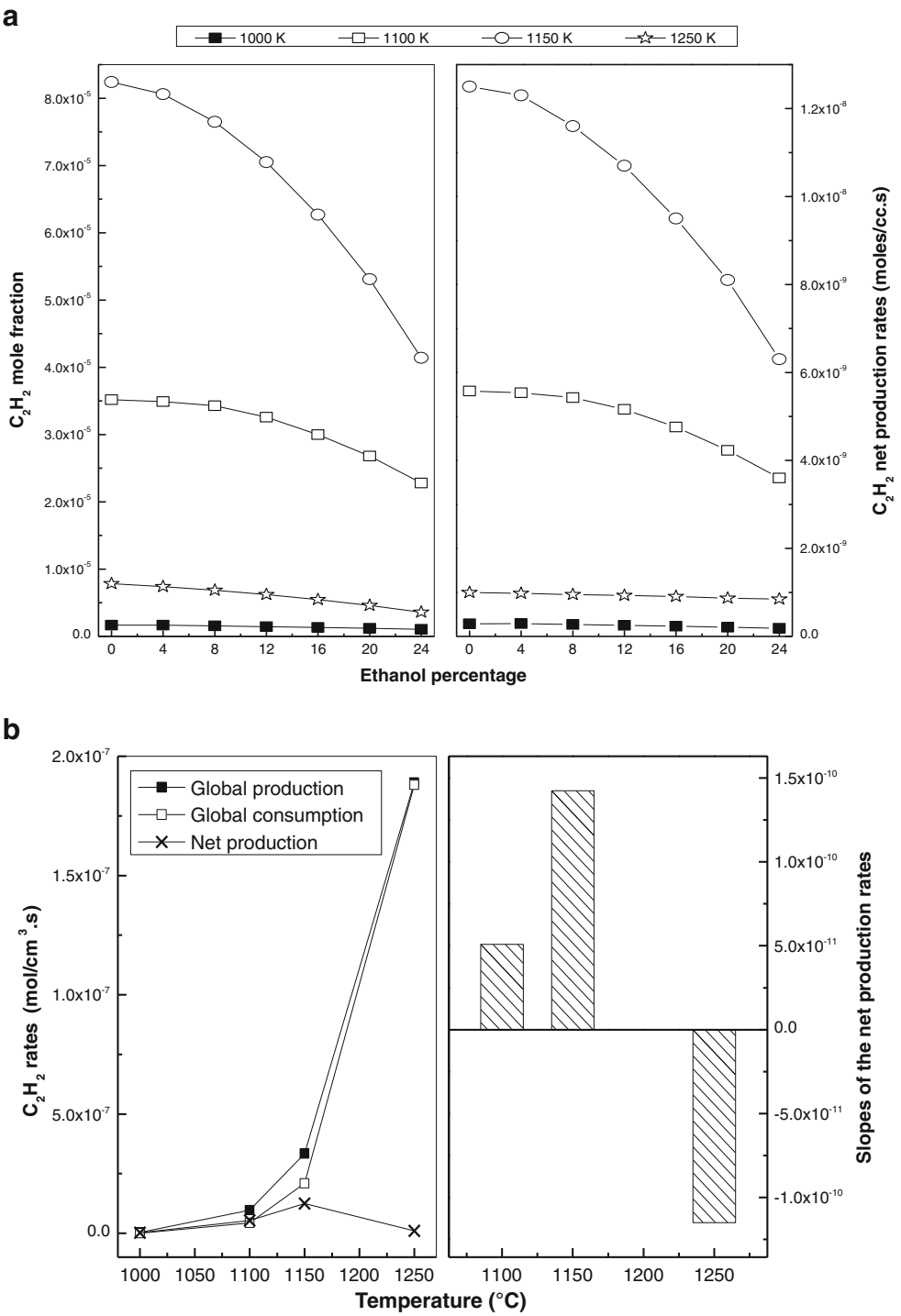

Fig. 3 **a** Effect of ethanol addition on acetylene mole fraction at different temperatures. **b** Variation of acetylene production, consumption, and net rates with reaction temperature in the neat benzene flame

fixed equivalence ratio, the fuel blended with methanol exhibited a peak concentration of acetylene 47 % lower than the one observed in the neat *n*-heptane flame. Same observations were also reported by Golea et al. (2012) during their modeling study on the effect of ethanol addition on the PAH and soot precursor concentrations in low-pressure (45-mbar) premixed benzene flames with an equivalence ratio of 2. Esarte et al. (2012) assessed gas and soot product concentrations during the pyrolysis of acetylene–alcohol (methanol, ethanol, isopropanol, or *n*-butanol) in a flow reactor in the 975–1,475-K temperature range. The authors reported that when alcohols are present in the reacting mixture, the final concentration of acetylene decreases at any temperature. It was postulated that the formation of radicals, such H and OH, that favor the consumption of acetylene was enhanced by the presence of the alcohols. Similar trends were observed by

Chen et al. (2012) during their study on the effects of adding oxygenated fuels to premixed *n*-heptane flames. Besides, Korobeinichev et al. (2011) reported during their study on the influence of ethanol on the process of forming soot precursors and PAH in ethylene flame at 30 Torr that the maximum of acetylene concentration dropped about 1.8 times in the ethanol–ethylene-blended flames as compared to the neat ethylene flame. In addition, in an extensive study focused on the intermediate-species pool, Wang et al. (2008) have recently investigated five pairs of propene–ethanol and propene–dimethyl ether (DME) flames with blends ranging from pure propene to pure oxygenate. The authors reported that the replacement of propene by ethanol led to a decrease in the peak mole fraction of C_2H_2. Furthermore, the investigation of the variation of PAH and soot mole fractions in a premixed laminar *n*-heptane flame with an equivalence ratio of 2 by adding methanol, ethanol, or methyl tertiary-butyl ether to the fuel showed that oxygenated mixtures displayed a significantly lower C_2H_2 concentrations as compared to the neat *n*-heptane flame (Inal and Senkan 2005). It was postulated that the oxygen in the additives remains connected to a carbon, which prevents that carbon from participating in any reactions of small, unsaturated species, thus reducing the mole fractions of low molecular weight reaction products. In contrast to these findings, when studying the effect of ethanol on the PAH and soot formation in five different one-dimensional, laminar, premixed ethanol–ethylbenzene flames, Therrien et al. (2010) reported that acetylene mole fractions exhibited increasing trends with increasing the ethanol amount in the fuel mixture. This finding was ascribed to the enhancement in the ethylene and ethane concentrations by the ethanol addition. These two species (ethylene and ethane) can decompose to form acetylene.

Our flux analysis results showed that acetylene (C_2H_2) formation pathways were dependent on ethanol proportion in the fuel mix. In neat benzene fuels, acetylene production was governed by the set of reactions:

$$C_2H_3 + C_2H_2 <=> C_4H_4 + H \quad (463)$$
$$C_2H_2 + C_2H_3 <=> C_4H_5\text{-}13 \quad (508)$$
$$a\text{-}C_3H_5 + C_2H_2 <=> c\text{-}C_5H_6 + H \quad (594)$$

The contribution of these reactions to the acetylene production was dependent on the reaction temperature. In the temperature range 1,100–1,250 K, the unimolecular decomposition of 1,3-butadienyl (C_4H_5-13) (508) was the most important reaction, and it displayed an increasing trend with a rise in the reaction temperature (at 1,100 K, the contribution of this reaction in the acetylene production was 33.4 %, whereas at 1,250 K, its contribution was 52 % which means a rise of 18.6 %). At a temperature of 1,000 K, the combination of the vinyl acetylene (C_4H_4) with hydrogen atoms (463) surpassed the reaction (508), and it accounted for 75.2 %. The rate of this reaction displayed a decreasing trend upon increasing the reaction temperature; the value at 1,250 K was 4.8 times less important than the one at 1,000 K.

In the case of ethanol-blended fuels, in addition to the above-mentioned reactions, the reaction of the vinyl radical (C_2H_3) with molecular oxygen ($C_2H_3+O_2<=>C_2H_2+HO_2$ (158)) played a crucial role in the acetylene formation. Its contribution was influenced by the ethanol proportion in the fuel mix as well as by the reaction temperature. Increasing the percentage of the oxygenate additive led to a rise in the rate of the reaction (508) (at 1,250 K, a rise of 1 % was observed in the case of fuels containing 24 % of ethanol as compared to the neat benzene fuel) and to a lowering in the rate of the reaction (463) (the rate was 14.1 % in the case of 24 % oxygen-blended fuels and 15.7 in the case of the neat benzene fuel which means a lowering of 1.6 %).

Finally, it is noteworthy that, regardless of the reaction temperature, the global rate of production (sum of all rates of production) was lowered upon increasing the ethanol amount in the fuel mix. It is well-known from the open literature that due to its strong C–H bond, acetylene has difficulty in undergoing abstraction reactions with radicals, as many hydrocarbons do (Abian et al. 2008; Alzueta et al. 2008; Laskin and Wang 1999). This species thus undergoes addition reactions generating intermediate adducts, followed by either reverse reaction or reaction into new different products (Abian et al. 2008; Alzueta et al. 2008). The initiation reactions for acetylene conversion, under the conditions of this work, include its interaction with the O, H, and OH radical pool and O_2:

$$C_2H_2 + O <=> TCH_2 + CO \quad (145)$$
$$C_2H_2 + O <=> HCCO + H \quad (146)$$
$$C_2H_2 + OH <=> CH_2CO + H \quad (148)$$
$$C_2H_2 + O_2 <=> HCCO + OH \quad (150)$$
$$C_2H_3(+M) <=> C_2H_2 + H(+M) \quad (153)$$

Under all conditions, the reaction (146) was found to be the most important consumption reaction. However, its rate was dependent on both ethanol concentrations and reaction temperature. Increasing the availability of the oxygenated additive led to a lower rate (at 1,000 K, a decrease of 18.4 % was observed in the case of 24 % oxygen-blended fuels as compared to the neat benzene fuel). The opposite behavior was observed upon raising the reaction temperature (in the neat benzene fuel, a rise of 37.5 % was observed at 1,250 K as compared to 1,000 K). On the other hand, the modeling results showed that all the other reactions evolved in the C_2H_2 consumption were of a comparatively medium scale. The rate of

the reaction (145) was independent on the blending compound (ethanol) level and displayed an increasing trend upon rising the reaction temperature, while the rate of the reaction (148) was boosted by boosting either the ethanol concentration in the fuel mix or the reaction temperature, whereas the rate of the reaction (150) exhibited an opposite behavior; it was lowered by increasing either the ethanol concentration or the reaction temperature. In addition, the rate of the reaction (153) was lowered upon increasing the reaction temperature, and it was enhanced by a rise in the ethanol concentration in the fuel mix.

Finally, it is noteworthy that, regardless of the reaction temperature, the global rate of consumption (sum of all rates of consumption) was lowered upon increasing the ethanol amount in the fuel mix. From these results, it is obvious that a decrease in both formation and consumption reactions of C_2H_2 was observed upon increasing the ethanol percentage in the fuel mixture. However, the net effect (global rate of production minus global rate of consumption) (see Fig. 3a) exhibited a decreasing trend upon increasing benzene replacement percentage by oxygenate additive, which means that the decrease in the formation reactions was more noticeable than the one of the consumption ones and consequently the C_2H_2 concentration decreased upon increasing the ethanol amount.

On the other hand, the flux analysis results showed that, regardless of the oxygenate additive percentage in the fuel mixture, the reaction temperature of 1,150 K displayed the maximum acetylene mole fraction (Fig. 3a). This finding may be ascribed to the fact that, in all cases, the global rate of production (sum of all rates of C_2H_2 production) as well as the global rate of consumption (sum of all rates of C_2H_2 consumption) were boosted upon increasing the temperature reaction (Fig. 3b). However, at 1,150 K, the rise in the production rates was more pronounced than the enhancement in the consumption ones (the slope in the net production was the most important at 1,150 K), and consequently, the C_2H_2 net production rate exhibited the maximum value at 1,150 K, which led to a maximum acetylene mole fraction.

Cyclopentadienyl radical (C_5H_5)

Figure 4a portrays the dependence of the cyclopentadienyl radical (C_5H_5) mole fractions on the ethanol percentage. It can clearly be seen that, whatever the reaction temperature, with increasing ethanol percentage, cyclopentadienyl radical mole fraction was lowered. Addition of oxygenate significantly reduced the mole fractions of C_5H_5 up to about 81 % with respect to the levels in the neat benzene fuel.

The modeling data showed clearly that, for both neat benzene and blended ethanol–benzene fuels, C_5H_5 was mainly produced by c-C_5H_6 (cyclopentadiene) and C_6H_5O (phenoxy radical) via the reactions:

$$\text{c-}C_5H_6 + H <=> C_5H_5 + H_2 \quad (597)$$
$$\text{c-}C_5H_6 + O <=> C_5H_5 + OH \quad (599)$$
$$\text{c-}C_5H_6 + OH <=> C_5H_5 + H_2O \quad (602)$$
$$C_6H_5O <=> C_5H_5 + CO \quad (674)$$

Cyclopentadiene (c-C_5H_6) and the phenoxy radical (C_6H_5O) contribution to the cyclopentadienyl radical (C_5H_5) formation was dependent on the reaction temperature as well as on the ethanol percentage. At a temperature of 1,000 K, the C_6H_5O contribution was 81.5 % in the neat benzene fuel and 59.5 % in the fuel blended with 24 % ethanol, whereas the c-C_5H_6 contribution was 18.5 and 40.5 % in the fuel containing 0 and 24 % ethanol, respectively. On the other hand, at a temperature of 1,250 K, C_6H_5O accounted for 56.6 and 49 %, whereas c-C_5H_6 accounted for 43.4 and 51 % for 0 and 24 % ethanol, respectively. In addition, the collected data showed that the rates of all these reactions were dependent on the reaction temperature as well as on the ethanol proportion in the fuel mix and that the global C_5H_5 rate of production displayed an increasing trend with a rise in the temperature reaction, whereas the opposite behavior was observed upon increasing the ethanol percentage.

Furthermore, it was found that, in the temperature range 1,000–1,150 K, the C_5H_5 depletion was governed by the set of reactions:

$$C_5H_5 + HO_2 <=> C_5H_5O + OH \quad (612)$$
$$C_5H_5 + O_2 <=> C_4H_4O + HCO \quad (613)$$
$$C_5H_5 + H <=> \text{c-}C_5H_6 \quad (605)$$
$$\text{c-}C_5H_6 + O_2 <=> C_5H_5 + HO_2 \quad (\text{Rev } 604)$$
$$C_5H_5 + O <=> C_4H_5\text{-}13 + CO \quad (606)$$

whereas, at 1,250 K, the C_5H_5 depletion was mainly due to the reactions:

$$C_5H_5 + H <=> \text{c-}C_5H_6 \quad (605)$$
$$C_5H_5 + O <=> C_4H_5\text{-}13 + CO \quad (606)$$
$$C_5H_5 + O <=> C_5H_5O \quad (607)$$

As in the case of production rates, all these reactions were dependent on the reaction temperature as well as on the ethanol proportion in the fuel mix. The global C_5H_5 rate of consumption was boosted by an increase in the temperature reaction, whereas the opposite trend was observed upon rising the ethanol percentage. It is noteworthy that the net rate of C_5H_5 production (global production rate−global consumption rate) was null whatever the reaction temperature and the ethanol proportion in the fuel mix, leading to the fact that

the cyclopentadienyl radical was in a quasi-stationary state. Thus, the observed decrease in the C_5H_5 mole fraction upon raising the ethanol concentration could not be interpreted by the net rate of production.

A snapshot of C_5H_5 formation–consumption paths, as given by means of the pathway analysis of the studied neat and blended fuels, is depicted in Fig. 4b. It can be seen that, at 1,000 K, in both neat benzene- and ethanol-blended fuels, the sequence reactions for the formation and consumption of the cyclopentadienyl radical (C_5H_5) were the same. However, the contribution of each reaction was dependent on the ethanol concentration. This observation suggests that ethanol does not change the C_5H_5 production–consumption scheme but it changes the pathway efficiency by varying the concentration of the pool radicals H, O, and OH. Same observations were observed at 1,250 K (figure not shown). To gain more insight on the influence of these radicals on the C_5H_5 formation–consumption, a sensitivity analysis was performed. The obtained results showed that the cyclopentadienyl radical mole fraction was dependent on c-C_5H_6, C_6H_5O, H, O, HO_2, O_2, and OH concentrations. By combining this result with the flux analysis results, it was concluded that the C_5H_5 mole fraction could be interpreted by using a ratio containing c-C_5H_6 and C_6H_5O mole fractions and the contributions of the production rates in the numerator as well as H, O, HO_2, O_2, and OH mole fractions and the contribution of the consumption rates in the denominator. Using this procedure, it was found that the C_5H_5 behavior could be interpreted by the ratio: $((a_i\ \text{c-}C_5H_6+b_i\ C_6H_5O)/(d_i\ H+e_i\ O+f_i\ HO_2+g_i\ O_2+h_i\ OH))$ where the coefficients a_i to h_i were constants dependent on the reaction temperature. From the results depicted in Fig. 4c, it can be clearly seen that, with increasing the ethanol percentage in the fuel mixture, H and OH mole fractions were increased, whereas O mole fractions were decreased; however, the lowering in the O concentrations was less noticeable than the rise in the H and OH concentrations, which means that the denominator, in the proposed ratio, was increased upon increasing the ethanol amount. On the other hand, a decrease was observed in both c-C_5H_6 and C_6H_5O mole fractions, which means that the increase in the ethanol proportion induced a decrease in the numerator of the proposed ratio; consequently, the ratio was lowered upon increasing the ethanol amount.

Propargyl radical (C_3H_3)

Concerning the propargyl radical (C_3H_3), the collected data showed that, in the case of reaction temperature of 1,000 K, a rise in the ethanol amount led to a rise in the mole fraction of the C_3H_3. The lowest value was obtained in the case of the 0 % oxygen fuel (1.8×10^{-9}), and the highest one was observed in the case of the 24 % oxygen fuel (2.02×10^{-9}) which means an increase of 12.2 %. In contrast, in the temperature range 1,100–1,250 K, the propargyl mole fractions were lowered upon increasing the ethanol concentration in the fuel mix. This lowering was the most noticeable in the case of 1,150 K: C_3H_3 radical mole fractions were the highest in the 0 % oxygen flame (2.9×10^{-8}) and the lowest in the 24 % oxygen flame (1.1×10^{-8}) which means a decrease of 62.1 % (Fig. 5a). This last finding is in qualitative agreement with the results reported by Golea et al. (2012) and by Korobeinichev et al. (2011) who observed a C_3H_3 concentration six times less important in ethanol-blended ethylene fuel as compared to the neat ethylene flame. Similar trends were also reported by Wang et al. (2008) when studying the effect of the ethanol addition on the combustion of propene. The authors mentioned that the C_3 intermediates were significantly diminished as propene was replaced by DME or ethanol. The maximum mole fractions for C_3H_3 decreased almost linearly down to the detection limit. At their turn, Gerasimov et al. (2012) when studying the effect of ethanol addition to unburnt gas mixture on the species pool in a fuel-rich flat, premixed, laminar ethylene flame at atmospheric pressure mentioned that the C_3H_3 maximum mole fraction in the flame with ethanol was approximately half that in the pure ethylene flame. In addition, a reduction of about 2.2–2.5 times in the C_3H_3 mole fraction was observed during a recent study by Frassoldati et al. (2011) for propene and propene/ethanol fuel-rich premixed flames at 40 mbar, when 50 % of propene were replaced with ethanol.

Pathway analysis results showed that in the case of 1,000 K, the predominant channels of C_3H_3 production were the three reactions:

$$C_3H_3 + H_2O <=> C_2H_3CHO + H \quad (317)$$
$$\text{p-}C_3H_4 + OH <=> C_3H_3 + H_2O \quad (343)$$
$$C_3H_3 + C_2H_2 <=> \text{l–}C_5H_5 \quad (633)$$

The contribution of the reaction (317) was 48 % in the neat benzene fuel and 63.6 % in the case of fuels containing 24 % of ethanol, which means an increase of 15.6 %. The reaction (343) showed an opposite trend; its contribution was 30.6 % in the neat benzene fuel and 14.5 % in the case of 24 % ethanol–benzene fuels, which means a decrease of 16.1 %. Besides, the reaction (633) accounted for 6.5 % in the case of fuels containing 0 % ethanol and for 8.5 % in the case of fuels containing 24 % ethanol. It is noteworthy that a rise in the ethanol amount induced a lowering in the C_3H_3 global production rate (sum of all production rates).

Fig. 4 **a** Effect of ethanol on cyclopentadienyl radical (C_5H_5) mole fraction at different temperatures. **b** Sequence reactions for the formation and consumption of cyclopentadienyl radical (C_5H_5). *A* At 1,000 K and 0 % ethanol; *B* at 1,000 K and 24 % ethanol. **c** Effect of ethanol addition on H, O, OH, c-C_5H_6, and C_6H_5O mole fractions at 1,000 K

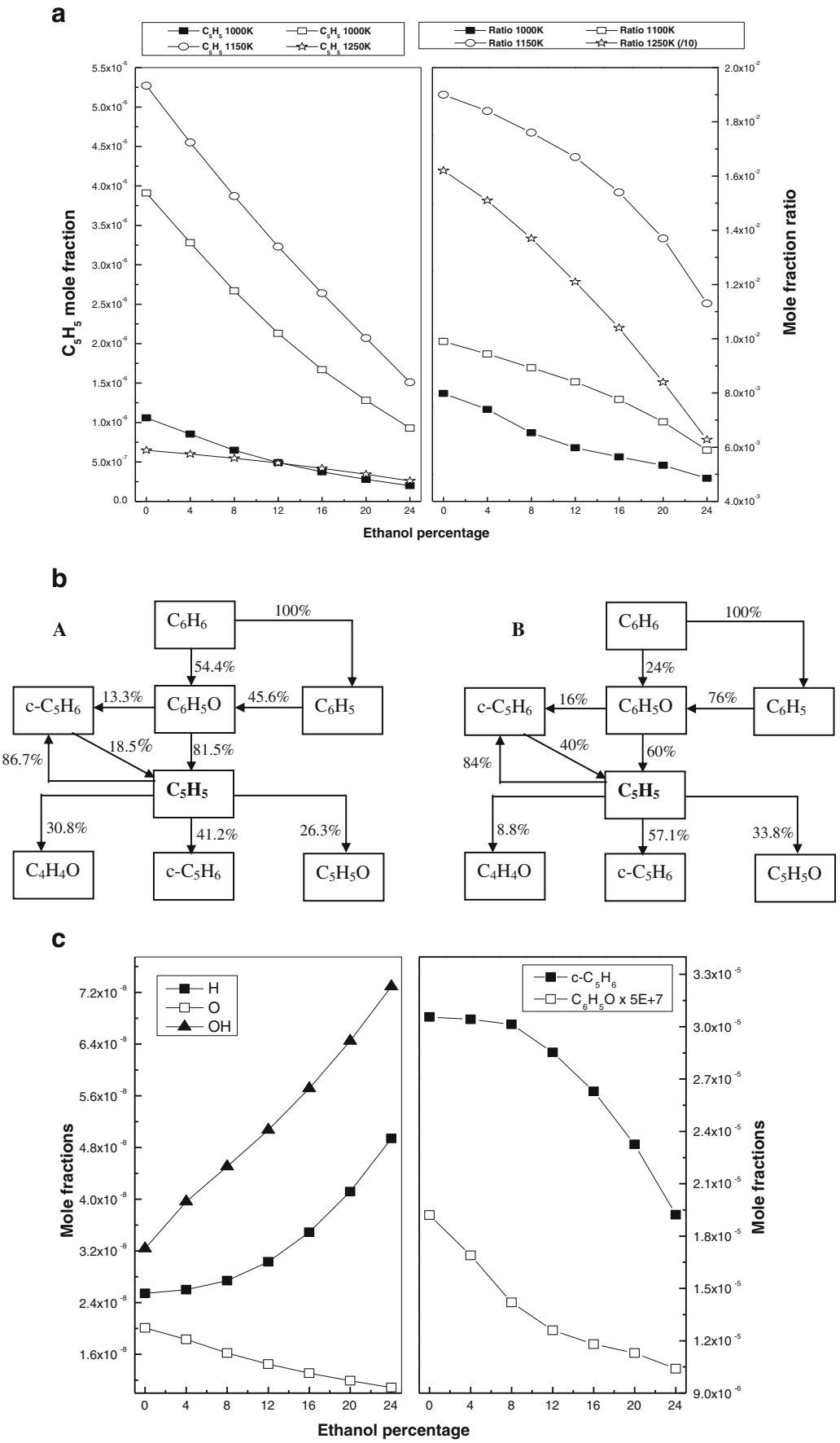
a
C5H5 1000K
C5H5 1000K
C5H5 1150K
C5H5 1250K
Ratio 1000K
Ratio 1100K
Ratio 1150K
Ratio 1250K (/10)
C5H5 mole fraction
Mole fraction ratio
Ethanol percentage
b
A
C6H6
100%
54.4%
c-C5H6
13.3%
C6H5O
45.6%
C6H5
18.5%
81.5%
86.7%
C5H5
30.8%
41.2%
26.3%
C4H4O
c-C5H6
C5H5O
B
C6H6
100%
24%
c-C5H6
16%
C6H5O
76%
C6H5
40%
60%
84%
C5H5
8.8%
57.1%
33.8%
C4H4O
c-C5H6
C5H5O
c
H
O
OH
c-C5H6
C6H5O x 5E+7
Mole fractions
Mole fractions
Ethanol percentage

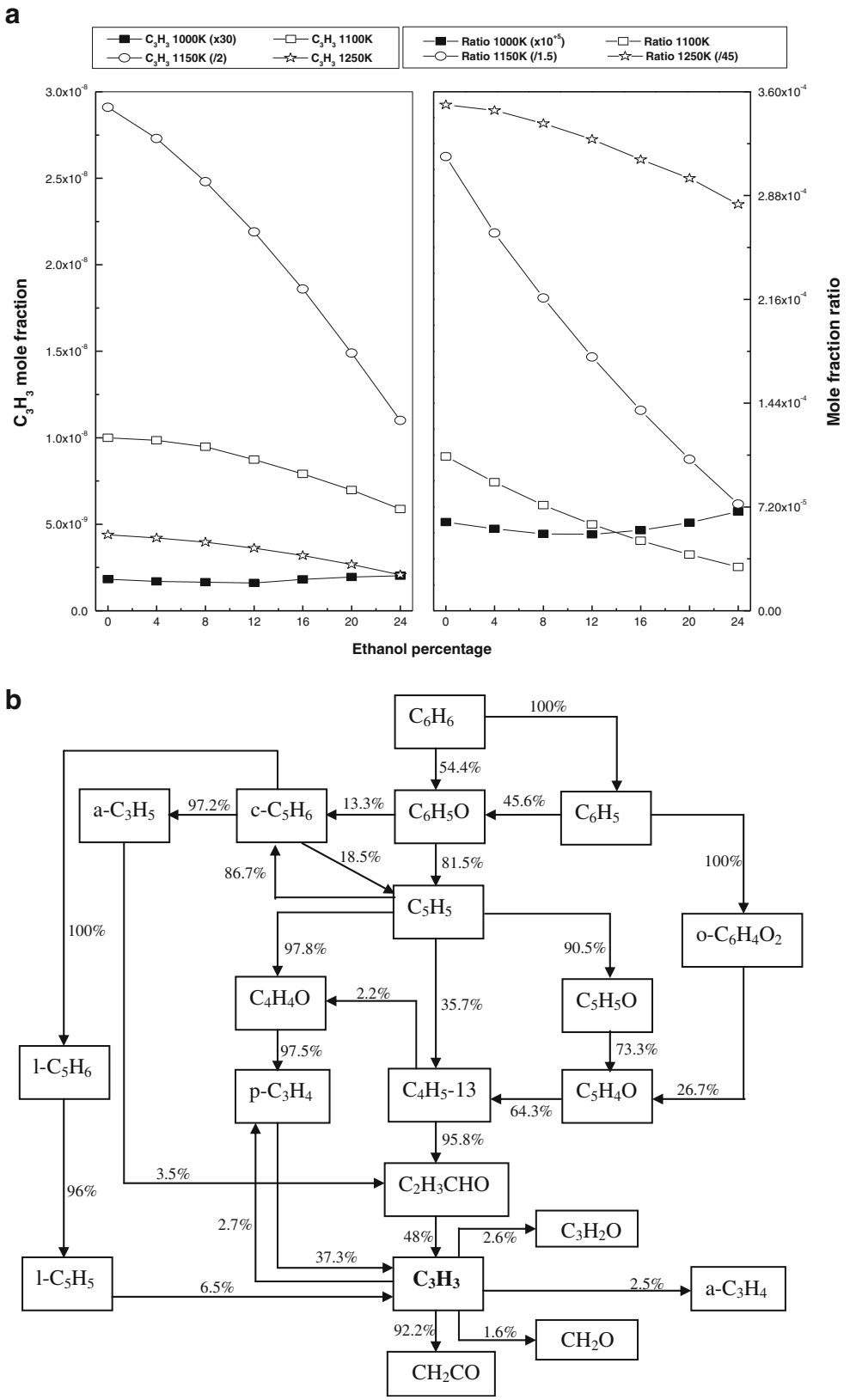

Fig. 5 **a** Effect of ethanol addition on propargyl radical (C_3H_3) mole fraction at different temperatures. **b** Sequence reactions for the formation and consumption of the propargyl radical (C_3H_3) at 1,000 K and 0 % ethanol. **c** Sequence reactions for the formation and consumption of the propargyl radical (C_3H_3) at 1,000 K and 24 % ethanol

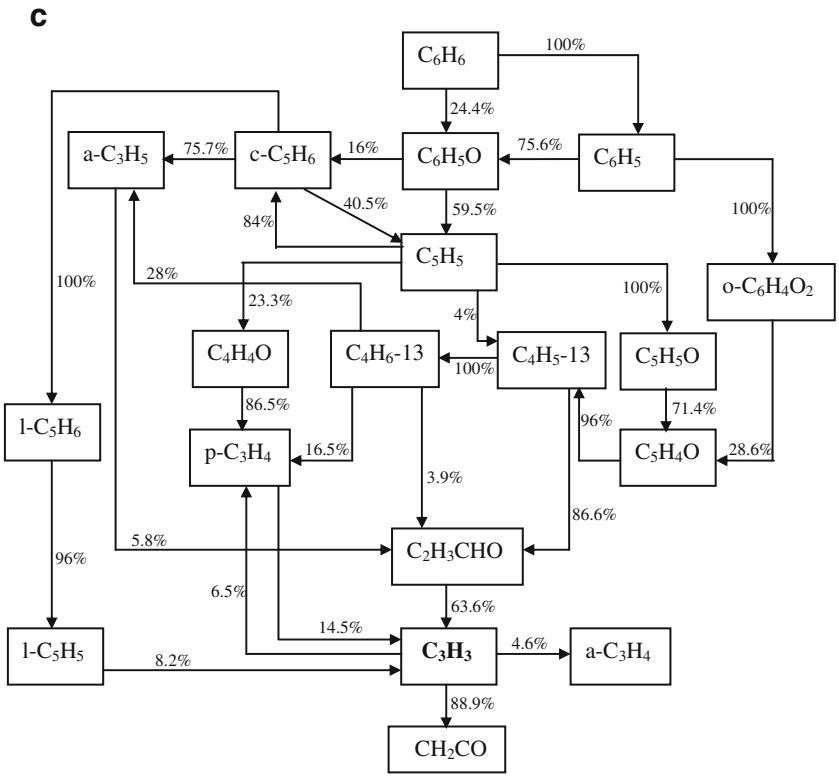

Fig. 5 (continued)

In addition, the obtained data showed that, at 1,000 K, the sole consumption reaction of the C_3H_3 radical was its attack by the molecular oxygen leading to ketene (CH_2CO) and formyl radical (HCO):

$$C_3H_3 + O_2 <=> CH_2CO + HCO \quad (316)$$

This reaction exhibited a decreasing trend with a rise in the ethanol amount in the fuel mix.

As in the case of cyclopentadienyl radical, it was found that, regardless the amount of the additive compound, the difference between the C_3H_3 global production and the rate of the reaction (316) was equal to zero, which means that also the propargyl radical was in the quasi-stationary state. Thus, also in this case, the observed rise in the C_3H_3 could not be interpreted by the net rate of production.

Snapshots of C_3H_3 formation–consumption paths, as given by means of the pathway analysis of the studied neat and blended fuels, are depicted in Fig. 5b, c. It can be seen that, at 1,000 K, in both neat benzene fuel- and ethanol-blended fuels, the sequence reactions for the formation and consumption of the propargyl radical (C_3H_3) were the same. However, the contribution of each reaction was dependent on the ethanol concentration. This observation suggests that ethanol does not change the C_3H_3 production–consumption scheme but it changes the pathway efficiency by varying the pool radicals concentrations as well as the C_3H_4 (a-C_3H_4 and p-C_3H_4) mole fractions. As in the case of C_5H_5, in order to gain more insight on the influence of these radicals on the C_3H_3 formation–consumption, a sensitivity analysis was performed. The collected data demonstrated that the propargyl mole fraction decrease, with an increase in the ethanol percentage, could be interpreted by the ratio: $((0.558\times[H]+0.288\times[p\text{-}C_3H_4])/0.9\times[O_2])$, noted as "ratio 1,000 K" (see Fig. 5a).

In the temperature range 1,100–1,250 K, the flux analysis showed that in addition to the reactions (317, 343, and 633) evolved in the C_3H_3 production at 1,000 K, three other reactions were found to have a noticeable effect on the production of the propargyl radical:

$$p\text{-}C_3H_4 + H <=> C_3H_3 + H_2 \quad (338)$$
$$p\text{-}C_3H_4 + CH_3 <=> C_3H_3 + CH_4 \quad (346)$$
$$C_4H_6\text{-}13 + C_3H_3 <=> C_4H_5\text{-}13 + p\text{-}C_3H_4 \quad (549)$$

Rates of the reactions (338) and (549) were found to be raised with a rise in the ethanol proportion in the fuel mix, whereas the reaction (346) rate displayed an opposite behavior. It is noteworthy that the global rate of C_3H_3 production, in the temperature range 1,100–1,250 K, was boosted upon increasing the ethanol proportion in the fuel mix.

On the other hand, it was found that, in the temperature range 1,100–1,250 K, the main C_3H_3 consumption reactions

were its attack by atomic oxygen, molecular oxygen, and hydrogen radical:

$$C_3H_3 + O <=> C_3H_2O + H \quad (314)$$
$$C_3H_3 + O_2 <=> CH_2CO + HCO \quad (316)$$
$$C_3H_3 + H + M <=> p\text{-}C_3H_4 + M \quad (349)$$
$$C_3H_3 + O <=> CH_2O + C_2H \quad (856)$$
$$C_3H_3 + H(+M) <=> a\text{-}C_3H_4(+M) \quad (859)$$

The rates of these reactions were dependent on both ethanol concentrations and temperature. The reactions (314, 316, and 856) exhibited a decreasing trend with increasing ethanol proportion in the fuel mix (a decrease of 100, 14.6, and 100 % was observed, at 1,100 K, for 314, 316, and 856, respectively), whereas the reactions (349 and 859) displayed an opposite behavior; they were boosted upon increasing the amount of the oxygenate additive in the mixture fuel (an increase of 62 and 60 % was observed, at 1,100 K, for 349 and 859, respectively). However, it should be mentioned that, as in the case of the global C_3H_3 production rate, the global C_3H_3 consumption rate (the sum of all consumption rates), in the temperature range 1,100–1,250 K, displayed an increasing trend with a rise in the ethanol concentration and that the net rate of the propargyl radical production was null whatever the temperature value, leading to the fact that the C_3H_3 was in the quasi-stationary state.

As in the case of the reaction temperature 1,000 K, to gain more insight in the C_3H_3 lowering with a rise in the ethanol proportion in the fuel mix, in the temperature range 1,100–1,250 K, a combination of flux analysis and sensitivity analysis results was used. It was found that the C_3H_3 decrease could always be interpreted by the ratio $((a_i\ p\text{-}C_3H_4 + b_i\ H + c_i\ a\text{-}C_3H_4)/(d_i\ O_2 + e_i\ O + f_i\ H + g_i\ a\text{-}C_3H_4))$ where the coefficients a_i to g_i were constants dependent on the reaction temperature. From the results depicted in Fig. 5a, it can be seen that, whatever the reaction temperature in the range 1,100–1,250 K, this ratio decreased upon increasing the amount of ethanol in the fuel mix.

Conclusions

In this paper, we report the effect of ethanol addition on the formation–consumption of some pollutants issued from the benzene oxidation in a jet-stirred reactor conditions. The most outstanding observations are:

- At all reaction temperatures, acetylene and cyclopentadienyl radical concentrations were decreased upon increasing the percentage of the ethanol in the mixture. This decrease was dependent on the reaction temperature.
- At 1,000 K, a rise in the ethanol induced an enhancement in the C_3H_3 mole fraction, whereas in the temperature range 1,100–1,250 K, the propargyl concentrations were lowered upon increasing the ethanol percentage in the fuel mix. This lowering was the most noticeable at 1,150 K, where a decrease of 62.1 % was observed.
- Pathway analysis demonstrated that ethanol did not change the cyclopentadienyl and propargyl radicals' production–consumption schemes but it changed the pathway efficiency by varying the concentration of the pool radicals H, O, and OH.

References

Abian M, Esarte C, Millera A, Bilbao R, Alzueta MU (2008) Oxidation of acetylene–ethanol mixtures and their interaction with NO. Energy Fuels 22:3814–3823

Aboussi B (1991) Etude Expérimentale et Modélisation de l'Oxydation de l'Ethanol. Dissertation, University of Orleans

Agarwal K (2007) Biofuels (alcohols and biodiesel) applications as fuels for internal combustion engines. Prog Energy Combust Sci 33:233–271

Alexiou A, Williams A (1996) Soot formation in shock-tube pyrolysis of toluene, toluene–methanol, toluene–ethanol, and toluene–oxygen mixtures. Combust Flame 104:51–65

Alzueta MU, Oliva M, Glarborg P (1998) Parabenzoquinone pyrolysis and oxidation in a flow reactor. Int J Chem Kinet 30:683–697

Alzueta MU, Glarborg P, Dam-Johansen K (2000) Experimental and kinetic modeling study of the oxidation of benzene. Int J Chem Kinet 32:498–522

Alzueta MU, Borruey M, Callejas A, Millera A, Bilbao R (2008) An experimental and modeling study of the oxidation of acetylene in a flow reactor. Combust Flame 152:377–386

Appel J, Bockhorn H, Frenklach M (2000) Kinetic modeling of soot formation with detailed chemistry and physics: laminar premixed flames of C2 hydrocarbons. Combust Flame 121:122–136

Arslan HE, Güneş D, Şenveli E, Doğru B (2012) Experimental investigation of the effect of using ethanol-blended diesel fuels on engine performance and exhaust emissions. Petrol Sci Technol 30:100–113

Balat M, Balat H, Oz C (2008) Progress in bioethanol processing. Prog Energy Combust Sci 34:551–573

Bennett BAV, McEnally CS, Pfefferle LD, Smooke MD, Colket MB (2009) Computational and experimental study of the effects of adding dimethyl ether and ethanol to nonpremixed ethylene/air flames. Combust Flame 156:1289–1302

Bittner JD, Howard JB (1981) Composition profiles and reaction mechanism in a near-sooting premixed benzene–oxygen–argon flame. Proc Combust Inst 28:1105–1116

Black G, Curran HJ, Pichon S, Simmie JM, Zhukov V (2010) Biobutanol: combustion properties and detailed chemical kinetic model. Combust Flame 157:363–373

Böhm H, Braun-Unkhoff M (2008) Numerical study of the effect of oxygenated blending compounds on soot formation in shock tubes. Combust Flame 153:84–96

Burcat A, Snyder C, Brabbs T (1986) Ignition delay times of benzene and toluene with oxygen in argon mixtures. NASA TM-87312

Celik MB (2008) Experimental determination of suitable ethanol–gasoline blend rate at high compression ratio for gasoline engine. Appl Therm Eng 28:396–404

Chai Y, Pfefferle LD (1998) An experimental study of benzene oxidation at fuel-lean and stoichiometric equivalence ratio conditions. Fuel 77:313–320

Chen G, Yu W, Fu J, Mo J, Huang Z, Yang J, Wang Z, Jin H, Qi F (2012) Experimental and modeling study of the effects of adding oxygenated fuels to premixed *n*-heptane flames. Combust Flame 159:2324–2335

Chen G, Yua W, Jiang X, Huang Z, Wang Z, Cheng Z (2013) Experimental and modeling study on the influences of methanol on premixed fuel-rich *n*-heptane flames. Fuel 103:467–472

Defoeux F, Dias V, Renard C, VanTiggelen PJ, Vandooren J (2005) Experimental investigation of the structure of a sooting premixed benzene/oxygen/argon flame burning at low pressure. Proc Combust Inst 30:1407–1415

Delshad AB, Raymond L, Sawicki V, Wegener T (2010) Public attitudes toward political and technological options for biofuels. Energ Policy 38:3414–3425

Detilleux V, Vandooren J (2009) Experimental study and kinetic modeling of benzene oxidation in one-dimensional laminar premixed low-pressure flames. Combust Explos Shock Waves 45:392–403

Dunphy MP, Simmie JM (1991) High-temperature oxidation of ethanol. Part 1: ignition delays in shock waves. J Chem Soc Faraday Trans 87:1691–1695

Emdee JL, Brezinsky K, Glassman I (1992) A kinetic model for the oxidation of toluene near 1200 K. J Phys Chem 96:2151–2161

Esarte C, Abian M, Millera A, Bilbao R, Alzueta MU (2012) Gas and soot products formed in the pyrolysis of acetylene mixed with methanol, ethanol, isopropanol or *n*-butanol. Energy 43:37–46

Fieweger K, Blumenthal R, Adomeit G (1997) Self-ignition of S.I. engine model fuels: a shock tube investigation at high pressure. Combust Flame 109:599–619

Francisco A M, Ahmad R G (2006) Performance and exhaust emissions of a single cylinder utility engine using ethanol fuel. SAE technical paper [2006-32-0078]

Frassoldati A, Cuoci A, Faravelli T, Ranzi E (2010) Kinetic modeling of the oxidation of ethanol and gasoline surrogate mixtures. Combust Sci Technol 182:653–667

Frassoldati A, Faravelli T, Ranzi E, Kohse-Höinghaus K, Westmoreland PR (2011) Kinetic modeling study of ethanol and dimethyl ether addition to premixed low-pressure propene–oxygen–argon flames. Combust Flame 158:1264–1276

Frassoldati A, Grana R, Faravelli T, Ranzi E, Oßwald P, Kohse-Höinghaus K (2012) Detailed kinetic modeling of the combustion of the four butanol isomers in premixed low-pressure flames. Combust Flame 159:2295–2311

Frenklach M, Warnatz J (1987) Detailed modeling of PAH profiles in a sooting low-pressure acetylene flame. Combust Sci Technol 51: 265–283

Gerasimov IE, Knyazkov DA, Yakimov SA, Bolshova TA, Shmakov AG, Korobeinichev OP (2012) Structure of atmospheric-pressure fuel-rich premixed ethylene flame with and without ethanol. Combust Flame 159:1840–1850

Glarborg P, Kee R J, Grcar J F, Mille, J A (1986) PSR: a FORTRAN program for modeling well-stirred reactors, SAND86-8209. Sandia National Laboratories, Livermore

Golea D, Rezgui Y, Guemini M, Hamdane S (2012) Reduction of PAH and soot precursors in benzene flames by addition of ethanol. J Phys Chem A 116:3625–3642

Gulder OL (1982) Laminar burning velocities of methanol, ethanol and iso-octane–air mixtures. Proc Combust Inst 19:275–281

Guo Z, Li T, Dong J, Chen R, Xue P, Wei X (2011) Combustion and emission characteristics of blends of diesel fuel and methanol-to-diesel. Fuel 90:1305–1308

He BQ, Shuai SJ, Wang JX, He H (2003) The effect of ethanol blended diesel fuels on emissions from a diesel engine. Atmos Environ 37: 4965–4971

Huang Z, Wang Q, Miao H, Wang X, Zeng K, Liu B, Jiang D (2007) Study on dimethyl ether–air premixed mixture combustion with a constant volume vessel. Energy Fuels 21:2013–2017

Huang J, Wang Y, Li S, Roskilly AP, Yu H, Li H (2009) Experimental investigation on the performance and emissions of a diesel engine fuelled with ethanol–diesel blends. Appl Therm Eng 29:2484–2490

Hwang JY, Lee W, Kang HG, Chung SH (1998) Synergistic effect of ethylene–propane mixture on soot formation in laminar diffusion flames. Combust Flame 114:370–380

Inal F, Senkan SM (2005) Effects of oxygenate concentration on species mole fractions in premixed *n*-heptane flames. Fuel 84:495–503

Johnson MV, Goldsborough SS (2009) A shock tube study of *n*- and iso-propanol ignition. Energy Fuels 23:5886–5898

Karavalakis G, Durbin TD, Shrivastava M, Zheng Z, Villela M, Jung H (2012) Impacts of ethanol fuel level on emissions of regulated and unregulated pollutants from a fleet of gasoline light-duty vehicles. Fuel 93:549–558

Keskin A, Gürü M (2011) The effects of ethanol and propanol additions into unleaded gasoline on exhaust and noise emissions of a spark ignition engine. Energy Sources A 33:2194–2205

Kim DH, Kim JK, Jang SH, Mulholland JA, Ryu JY (2007) Thermal formation of polycyclic aromatic hydrocarbons from cyclopentadiene (CPD). Environ Eng Res 12:211–217

Knothe G (2010) Biodiesel and renewable diesel: a comparison. Prog Energy Combust Sci 36:364–373

Kohse-Hoinghaus K, Oßwald P, Cool TA, Kasper T, Hansen N, Qi F, Westbrook CK, Westmoreland PR (2010) Biofuel combustion chemistry: from ethanol to biodiesel. Angew Chem Int Ed 49: 3572–3597

Korobeinichev OP, Yakimov SA, Knyazkov DA, Bolshova TA, Shmakov AG, Yang J, Qi F (2011) A study of low-pressure premixed ethylene flame with and without ethanol using photoionization mass spectrometry and modeling. Proc Combust Inst 33:569–576

Lapuerta M, Armas O, Herreros JM (2008) Emissions from a diesel–bioethanol blend in an automotive diesel engine. Fuel 87:25–31

Laskin A, Wang H (1999) On initiation reactions of acetylene oxidation in shock tubes. A quantum mechanical and detailed kinetic modeling study. Chem Phys Lett 303:43–49

Lee SM, Yoon SS, Chung SH (2004) Synergistic effect on soot formation in counterflow diffusion flames of ethylene–propane mixtures with benzene addition. Combust Flame 136:493–500

Li J, Kazakov A, Dryer FL (2001) Ethanol pyrolysis experiments in a variable pressure flow reactor. Int Chem Kin 33:859–867

Li J, Zhao Z, Kazakov A, Chaos M, Dryer FL, Scire JJ (2007) A comprehensive kinetic mechanism for CO, CH2O, and CH3OH combustion. Int J Chem Kinet 39:109–136

Liang G, Yan YY, Manzhi T, Hua L, Yaping P (2011) An experimental study on improving the ignition of ethanol–diesel blended fuel (EDBF). Chem Eng Comm 198:1263–1274

Lin WY, Chang YY, Hsieh YR (2010) Effect of ethanol–gasoline blends on small engine generator energy efficiency and exhaust emission. J Air Waste Manage Assoc 60:142–148

Litzinger T, Colket M, Kahandawala M, Katta V, Lee SY, Liscinsky D, McNesby K, Pawlik R, Roquemore M, Santoro R, Sidhu S, Stouffer S, Wu J (2009) Fuel additive effects on soot across a suite of laboratory devices, part 1: ethanol. Combust Sci Technol 181:310–328

Lovell AB, Brezinsky K, Glassman I (1989) The gas phase pyrolysis of phenol. Int J Chem Kinet 21:547–560

Maricq MM, Szente JJ, Jahr K (2012) The impact of ethanol fuel blends on PM emissions from a light-duty GDI vehicle. Aerosol Sci Technol 46:576–583

Marinov NM (1999) A detailed chemical kinetic model for high temperature ethanol oxidation. Int J Chem Kinet 31:183–220

Marriott CD, Wiles MA, Gwidt JM, Parrish SE (2008) Development of a naturally aspirated spark ignition direct-injection flex-fuel engine. SAE technical paper [2008-01-0319]

McEnally CS, Pfefferle LD (1998) An experimental study in non-premixed flames of hydrocarbon growth processes that involve five-membered carbon rings. Combust Sci Technol 131:323–344

Melius CF, Colvin ME, Marinov NM, Pitz WJ, Senkan SM (1996) Reaction mechanism in aromatic hydrocarbon formation involving the C_5H_5 cyclopentadienyl moiety. Proc Combust Inst 26:685–692

Miller JA, Melius CF (1992) Kinetic and thermodynamic issues in the formation of aromatic compounds in flames of aliphatic fuels. Combust Flame 91:21–39

Norton TS, Dryer FL (1992) An experimental and modeling study of ethanol oxidation kinetics in an atmospheric pressure flow reactor. Int J Chem Kinet 24:319–344

Palit S, Chodhuri AK, Mandal BK (2011) Environmental impact of using biodiesel as fuel in transportation: a review. Int J Glob Warm 3:232–256

Parag S, Raghavan V (2009) Experimental investigation of burning rates of pure ethanol and ethanol blended fuels. Combust Flame 156:997–1005

Pidol L, Lecointe B, Starck L, Jeuland N (2012) Ethanol–biodiesel–diesel fuel blends: performances and emissions in conventional diesel and advanced low temperature combustions. Fuel 93:329–338

Ristori A, Dagaut P, El Bakali A, Pengloan G, Cathonnet M (2001) Benzene oxidation: experimental results in a JSR and comprehensive kinetic modeling in JSR, shock-tube and flame. Combust Sci Tech 167:223–256

Salamanca M, Sirignano M, Commodo M, Minutolo P, D'Anna A (2012) The effect of ethanol on the particle size distributions in ethylene premixed flames. Exp Therm Fluid Sci 43:71–75

Sayin C, Uslu K (2008) Influence of advanced injection timing on the performance and emissions of CI engine fueled with ethanol-blended diesel fuel. Int J Energy Res 32:1006–1015

Sukjit E, Herreros JM, Dearn KD, García-Contreras R, Tsolakis A (2012) The effect of the addition of individual methyl esters on the combustion and emissions of ethanol and butanol–diesel blends. Energy 42:364–374

Tan Y, Frank P (1996) A detailed comprehensive kinetic model for benzene oxidation using the recent kinetic results. Proc Combust Inst 26:677–684

Therrien RJ, Ergut A, Levendis YA, Richter H, Howard JB, Carlson JB (2010) Investigation of critical equivalence ratio and chemical speciation in flames of ethylbenzene–ethanol blends. Combust Flame 157:296–312

Veloo PS, Wang YL, Egolfopoulos FN, Westbrook CK (2010) A comparative experimental and computational study of methanol, ethanol, and *n*-butanol flames. Combust Flame 157:1989–2004

Vourliotakis G, Skevis G, Founti MA (2011) A detailed kinetic modeling study of benzene oxidation and combustion in premixed flames and ideal reactors. Energy Fuels 25:1950–1963

Wang H, Frenklach M (1997) A detailed kinetic modeling study of aromatics formation in laminar premixed acetylene and ethylene flames. Combust Flame 110:173–221

Wang D, Violi A, Kim DH, Mullholland JA (2006) Formation of naphthalene, indene, and benzene from cyclopentadiene pyrolysis: a DFT study. J Phys Chem A 110:4719–4725

Wang J, Struckmeier U, Yang B, Cool TA, Osswald P, Kohse-Hoinghaus K, Kasper T, Hansen N, Westmoreland PR (2008) Isomer-specific influences on the composition of reaction intermediates in dimethyl ether/propene and ethanol/propene flame. J Phys Chem A 112:9255–9265

Yang B, Huang C, Wei L, Wang J, Sheng L, Zhang Y, Qi F, Zheng W, Li WK (2006) Identification of isomeric C_5H_3 and C_5H_5 free radicals in flame with tunable synchrotron photoionization. Chem Phys Lett 423:321–326

Yang B, Li Y, Wei L, Huang C, Wang J, Tian Z, Yang R, Sheng L, Zhang Y, Qi F (2007) An experimental study of the premixed benzene/oxygen/argon flame with tunable synchrotron photoionization. Proc Combust Inst 31:555–563

Yoon SH, Lee CS (2012) Effect of undiluted bioethanol on combustion and emissions reduction in a SI engine at various charge air conditions. Fuel 97:887–890

Yoon SS, Anh DH, Chung SH (2008a) Synergistic effect of mixing dimethyl ether with methane, ethane, propane, and ethylene fuels on polycyclic aromatic hydrocarbon and soot formation. Combust Flame 154:368–377

Yoon SH, Park SH, Lee CS (2008b) Experimental investigation on the fuel properties of biodiesel and its blends at various temperatures. Energy Fuels 22:652–656

Zhu L, Cheung CS, Zhang WG, Huang Z (2010) Emissions characteristics of a diesel engine operating on biodiesel and biodiesel blended with ethanol and methanol. Sci Total Environ 408:914–921